JOURNAL OF VIROLOGY, Jan. 1996, p. 298–304 Vol. 70, No. 1
0022-538X/96/$04.00+0

Lipid Membrane Fusion Induced by the Human Immunodeficiency Virus Type 1 gp41 N-Terminal Extremity Is Determined by Its Orientation in the Lipid Bilayer

ISABELLE MARTIN,[1]* HEINER SCHAAL,[2] ANDREAS SCHEID,[2] AND JEAN-MARIE RUYSSCHAERT[1]

Laboratoire de Chimie-Physique des Macromolécules aux Interfaces, Université Libre de Bruxelles, 1050 Brussels, Belgium,[1] and Biologisch-Medizinisches Forschungszentrum und Institut für Medizinische Mikrobiologie und Virologie, Heinrich-Heine-Universität Düsseldorf, D-40225 Düsseldorf, Germany[2]

Received 13 July 1995/Accepted 2 October 1995

The amino-terminal extremity of the human immunodeficiency virus type 1 transmembrane protein (gp41) is thought to play a pivotal role in the fusion of virus membranes with the plasma membrane of the target cell and in syncytium formation. Peptides with sequences taken from the human immunodeficiency virus type 1 gp41 fusogenic (synthetic peptides SPwt and SP-2) and nonfusogenic (SP-3 and SP-4) glycoproteins adopt mainly a β-sheet conformation in the absence of lipid, as determined by attenuated total reflection Fourier transform infrared spectroscopy, and after interaction with large unilamellar liposomes, the β-sheet is partly converted into an α-helical conformation. Peptides SPwt and SP-2 but not SP-3 or SP-4 were able to promote lipid mixing as assessed by fluorescence energy transfer assay and dye leakage in a vesicle leakage assay. By using polarized attenuated total reflection Fourier transform infrared spectroscopy, SPwt and SP-2 were found to adopt an oblique orientation in the lipid membrane whereas SP-3 and SP-4 were oriented nearly parallel to the plane of the membrane. These findings confirm the correlation between the membrane orientation of the α-helix and the lipid mixing ability in vitro. Interestingly, the data provide a direct correlation with the fusogenic activity of the parent glycoproteins in vivo.

The human immunodeficiency virus type 1 (HIV-1) envelope glycoprotein precursor gp160 is proteolytically cleaved by a cellular enzyme into a surface glycoprotein (gp120) and a transmembrane glycoprotein (gp41). This cleavage generates in gp41 the exposure of an N-terminal highly hydrophobic amino acid stretch, which has been proposed to interact with the lipid membrane during the fusion event. Involvement of the N termini of the glycoproteins of different enveloped viruses has been confirmed by mutational analysis: mutations which disrupt the distribution of the hydrophobic amino acids in the N terminus of the influenza virus hemagglutinin (HA) (8), gp41 of HIV-1 (5, 16, 29), and gp32 of simian immunodeficiency virus (SIV) (1) inhibit syncytium formation in transfected cells. The mode of interaction of the fusion peptide with the lipid membrane, in particular the mechanism of insertion into the membrane and the mechanism by which this facilitates the fusion between membranes, is not fully understood. The available evidence suggests that peptide hydrophobicity is important but that other factors such as the distribution of the amino acids on a helical motif are also involved, as well as the orientation of the peptide at the lipid/water interface (7, 14, 22, 35).

A possible way to elucidate the molecular mechanism of membrane fusion is to study the interaction of synthetic peptides corresponding to the amino terminus of viral fusion proteins with model membranes. Synthetic peptides corresponding to the N-terminal segment of the influenza virus HA_2 (18, 24, 27, 34) have been shown to interact with the lipid bilayer and to promote fusion of lipid vesicles. Similar observations have been made with SIV and HIV-1 fusion peptides (20, 25, 26).

In an attempt to establish a relationship between peptide fusion activity, structure, and orientation, we have recently investigated in a liposomal system the activity of a 12-residue synthetic peptide corresponding to the N-terminal extremity of SIV gp32 and modified SIV fusion peptides and have found that the oblique membrane insertion of the SIV fusion peptide is an essential requirement for membrane fusion (22). It is likely that this oblique orientation alters the parallelism between the phospholipid acyl chains, giving rise to new lipid phases which we now think to be associated with the initial events of membrane fusion.

Using an expression vector for the HIV-1 glycoprotein, Schaal et al. (29) have recently identified several deletions in the HIV-1 gp41 fusion peptide which abolish syncytium formation of transfected cells. In the present study, we asked whether the same mutations, when introduced into synthetic peptides, lead to corresponding changes in their physical interactions with membrane lipids and whether we can validate the correlation between peptide orientation and fusogenic activity. To correlate the activity of synthetic peptides with the activity of mutant glycoprotein, three mutant peptides corresponding in sequence to the N-terminal extremity of one active glycoprotein lacking two amino acids (SP-2) and two inactive glycoproteins lacking three and four amino acids (SP-3 and SP-4) were compared with a peptide with the wild-type sequence (SPwt). The membrane activity of the peptides in vitro conforms with the fusion activity of the parent glycoprotein. The presence or absence of fusion activity is correlated with the orientation of the peptides in the lipid bilayer established by Fourier transform infrared spectroscopy (FTIR).

MATERIALS AND METHODS

Materials. Egg phosphatidylethanolamine (PE) and egg phosphatidylcholine (PC) were purchased from Sigma Chemical Co., St. Louis, Mo. *N*-(Nitrobenzo-2-oxa1,3-diazol)phosphatidylethanolamine (NBD-PE) and *N*-(lissamine rhoda-

* Corresponding author. Mailing address: Université Libre de Bruxelles, Campus Plaine CP 206/2, B-1050 Bruxelles, Belgium. Phone: 32-02-650.53.66. Fax: 32-02-650.51.13.

mine B sulfonyl)phosphatidylethanolamine (Rh-PE) were from Avanti Polar Lipids Inc., Birmingham, Ala. 8-Aminonaphthalene-1,3,6-trisulfonic acid sodium salt and *p*-xylylenebis(pyridinium) bromide were from Molecular Probes Inc., Junction City, Oreg.

Calcein (Sigma) was purified by chromatography on Sephadex LH-20 (Pharmacia). Calcein was loaded on the column as a sodium salt solution and eluted with water at neutral pH. The concentration of calcein was determined spectrophotometrically by using 7.0×10^4 as the molar extinction coefficient at 492 nm (12).

High-pressure liquid chromatography-purified synthetic peptides in their amide form were purchased from Quality Controlled Biochemical, Inc., Hopkinton, Mass.

Vesicle preparation. Multilamellar vesicles (MLV) were obtained by vortexing a lipid film in Tris buffer (10 mM Tris, 150 mM NaCl, 0.1 mM EDTA, 0.02% NaN_3 [pH 7.4]). Large unilamellar vesicles (LUV) were prepared by the extrusion procedure of Hope et al. (13) with an extruder (Lipex Biomembranes Inc., Vancouver, Canada). Briefly, frozen and thawed MLV were extruded 10 times through two stacked polycarbonate membranes with a pore size of 0.1 μm (Nuclepore Corp., Pleasanton, Calif.).

Lipid mixing. Lipid mixing was determined by measuring the fluorescence intensity change resulting from the fluorescence energy transfer between two probes, NBD-PE and Rh-PE, inserted into the lipid bilayer, as described by Struck et al. (30). Fluorescence was monitored with a model 8000 spectrofluorimeter (SLM Instruments Inc., Urbana, Ill.) with excitation and emission slits of 4 nm. Probes were added to the lipid film, and LUV were prepared as described above. Liposomes containing both probes at 0.6% (molar ratio) each were mixed with probe-free liposomes at a 1:9 molar ratio and a final lipid concentration of 3×10^{-4} M. The initial fluorescence of the 1:9 (labeled/unlabeled) suspension was taken as 0% fluorescence, and the 100% fluorescence value was determined with an equivalent concentration of vesicles prepared with 0.06% of each fluorescent phospholipid. The suspensions were excited at 470 nm, and the NBD fluorescence was recorded at 530 nm.

Vesicle leakage assay. Dry lipid films were rehydrated to a concentration of 20 mg/ml in 10 mM *N*-2-hydroxyethylpiperazine-*N'*-2-ethanesulfonic acid (HEPES) buffer (pH 7.2) containing 62 mM calcein purified as described in Materials and Methods. Unencapsulated dye was removed by passing the liposome preparation over a Sephadex G-50 gel filtration column equilibrated with 10 mM HEPES–150 mM NaCl–1 mM EDTA buffer (pH 7.2). The liposome concentration was estimated by measuring the phosphorus content in the lipids (23). Release of the fluorescent dye from preloaded LUV at a final lipid concentration of 3×10^{-4} M was monitored with an SLM 8000 spectrofluorimeter. Experiments were conducted in a 1-ml stirred cuvette with right-angle illumination. Excitation and emission wavelengths were set at 490 and 520 nm, respectively, with a slit width of 4 nm. The addition of Triton X-100 to a final concentration of 0.1% (vol/vol) was used to determine maximal release. The percentage of total fluorescence was defined as $\% F_t = [(I_t - I_0)/(I_{100} - I_0)] \times 100$, where I_0 is the initial fluorescence, I_{100} is the total fluorescence observed after addition of Triton X-100, and I_t is the fluorescence observed after addition of fusion peptide at $t = 600$ s, corrected for dilution.

Attenuated total reflection (ATR)-FTIR. Spectra were recorded at room temperature on a Perkin-Elmer 1720X FTIR spectrophotometer equipped with a liquid nitrogen-cooled mercury-cadmium-telluride detector at a nominal resolution of 4 cm^{-1} and encoded every 1 cm^{-1}. The spectrophotometer was continuously purged with air dried on a silica gel column (5 by 130 cm). The internal reflection element was a germanium plate (50 by 50 by 2 mm; Harrick EJ2121) with an aperture angle of 45°, yielding 25 internal reflections. For each spectrum, 128 scan cycles were averaged; in each cycle, the ratio of the sample spectra with respect to the background spectra of a clean germanium plate was measured, using a shuttle to move the sample or reference into the beam. For polarization experiments, a Perkin-Elmer gold wire grid polarizer was positioned before the sample and the reference.

Samples were prepared by adding HIV-1 peptides, dissolved in dimethyl sulfoxide (DMSO) at a final concentration of 1 mg/ml, to liposomes (LUV PC/PE, 1:1) at various molar lipid/peptide ratios. After a 1-h incubation at 37°C, the lipid-peptide complex was separated from the free peptides on a Sephadex G-50 column (Pharmacia). Oriented multilayers were obtained by slow evaporation of the liposomes under an N_2 stream and at room temperature (9) on one side of the germanium plate. To differentiate between the α-helix and the random structures, the multilayers were exposed for 3 h to D_2O-saturated N_2 (2).

Determination of the secondary structure was based on the vibrational bands of protein or peptide, particularly the amide I band (1,600 to 1,700 cm^{-1}), which are sensitive to the secondary structure (6). This amide I band, located in a region of the spectrum often free of other bands, is made of 80% pure C═O vibration (11). The strong overlapping of the different components of the amide I arising from the different secondary structures usually results in a broad, featureless envelope. The combination of resolution enhancement methods with a band-fitting procedure allows the quantitative assessment of various components of protein or peptide secondary structure such as α-helix, β-sheet, and unordered structures (15, 31). Each band was assigned to a secondary structure according to the frequency of its maximum. The areas of all bands assigned to a given secondary structure were then summed and divided by the total area. This ratio gives the proportion of the polypeptide chain in that conformation. This procedure, extended to a series of well-characterized proteins, provided a correct estimation of the α-helix and β-sheet structure content with a standard deviation of 8.7% when X-ray structures were taken as the reference (9). The percentages of the different secondary structures were quantified by an iterative curve fitting. The frequency limits for each structure were first assigned according to data determined theoretically (17) or experimentally (31): 1,662 to 1,645 cm^{-1}, α-helix; 1,689 to 1,682 cm^{-1} and 1,637 to 1,613 cm^{-1}, β-sheet; 1,644.5 to 1,637 cm^{-1}, random; 1,682 to 1,662.5 cm^{-1}, β-turns. These limits have been slightly adjusted to obtain a good agreement between the proportion of each structure determined by ATR-FTIR and X-ray crystallography (9).

SPwt (16 aa)	AVGIGALFLGFLGAAG
SPwt.13 (13 aa)	AVGIGALFLGFLG
SIVwt (16 aa)	GVFVLGFLGFLATAGS
SIVwt.12 (12 aa)	GVFVLGFLGFLA
SP-2	A IGALFLGFLGAAG
SP-3	A GALFLGFLGAAG
SP-4	A ALFLGFLGAAG

FIG. 1. Amino acid sequences of synthetic peptides (SP) corresponding to the gp41 N terminus of HIV-1 (strain HIV_{NL43}) and deletion mutants (29). For comparison, analogous fusion-active SIV peptides of comparable length used in a previous study (20) are also depicted. aa, amino acids.

ATR-IR allows spectra to be recorded on ordered lipid bilayers and information to be gained about the orientation of different structures of protein or peptide (9, 10). In an α-helix, the main transition dipole moment (C═O) is almost parallel to the helix axis, while in an antiparallel β-sheet, the polarization is opposite, predominantly perpendicular to the fiber axis (11). It is therefore possible to determine the mean orientation of the α-helix and β-sheet structures from the orientation of the peptide bond corresponding to the C═O group. Spectra were recorded with parallel (0°) and perpendicular (90°) polarized incident light with respect to the ATR plate. Polarization was expressed as the dichroic ratio $R_{atr} = A_{90°}/A_{0°}$. The mean angle between the C═O bond and a normal to the ATR plate surface is calculated from R_{atr} as described by Cabiaux et al. (2).

The difference spectra are obtained by subtracting the 0° from the 90° polarization spectrum normalized to each other by setting to zero the net integral of the intensities of the ester C═O stretching band of the Sn-1 and Sn-2 lipid chains in the 1,710- to 1,760-cm^{-1} region in the difference spectrum. The rationale behind this lies in the fact that both the Sn-1 and Sn-2 carbonyl groups are found to make angles with respect to the bilayer normal that are close to the value for an isotropic orientation, and their IR intensities are therefore expected to be independent of the polarization.

RESULTS

Peptide-induced lipid mixing and dye leakage. The 16-amino-acid synthetic peptide (SPwt) corresponding to the fusogenic sequence of the HIV-1 gp41 has been shown to promote the lipid mixing of PE-containing LUV (PE/PC molar ratio = 1:1) (19) as determined by resonance energy transfer (30). Here, we compared three peptides corresponding to deletion mutants of the HIV-1 gp41 N-terminal extremity with SPwt (Fig. 1). Like SPwt, SP-2 promoted the fusion of LUV at a lipid/peptide molar ratio of 25, neutral pH, and 37°C. No fusion occurred with SP-3 and SP-4 under the same experimental conditions (Fig. 2A). This loss of fusion activity with deletions at the N terminus is not likely to be due to the decrease in the overall lengths of the inactive 12- and 13-amino-acid peptides, because a 13-amino-acid peptide resulting from the C-terminal deletion of the 16-amino-acid HIV fusion peptide showed a high fusion activity, as did a 12-amino-acid peptide of the analogous SIV fusion peptide (20) (Fig. 2A).

It has been shown in vivo that the cotransfection of a nonfusogenic mutant protein with the fusogenic wild-type gp41 resulted in a reduced cell-fusing activity of HeLa-$T4^+$ cells (29). We have therefore analyzed the capacity of the nonfusogenic peptides SP-3 and SP-4 to interfere with the activity of

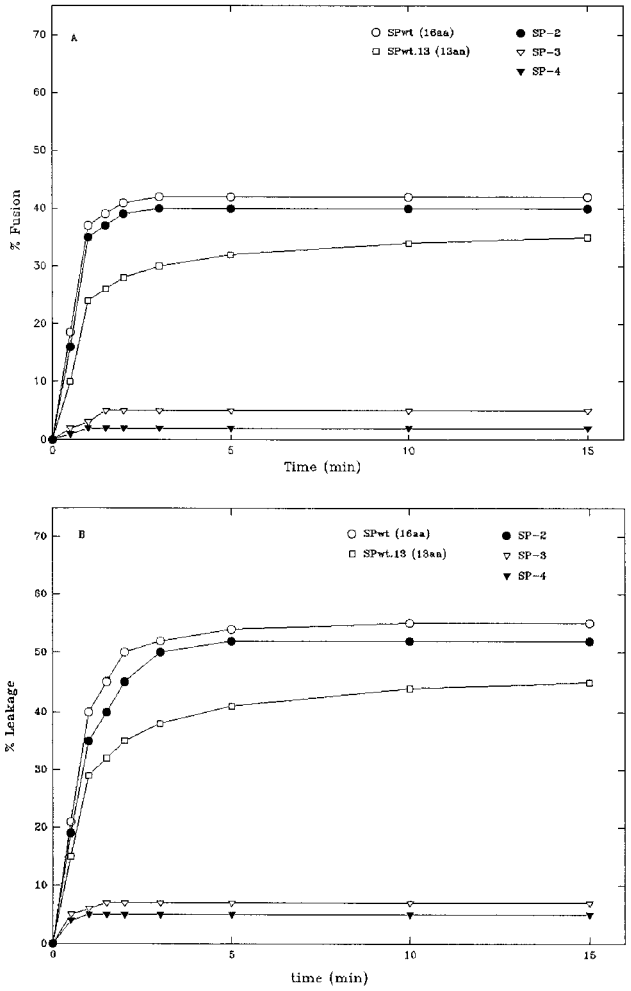

FIG. 2. Lipid mixing (A) and dye leakage (B) of LUV (PC/PE molar ratio, 1:1) induced by SPwt and mutant peptides. At time zero, the peptide dissolved in DMSO was added, and the decrease in fluorescence energy transfer following liposome-liposome fusion was monitored at 530 nm, pH 7.4, and 37°C. DMSO up to 2% (vol/vol), which is the maximal concentration used, did not modify the fluorescence. The total lipid concentration was 3×10^{-4} M, and the peptide concentration was 1.3×10^{-5} M.

the fusogenic peptides SPwt and SP-2. Addition to the vesicles of SPwt premixed with SP-3 or SP-4 at a 1:1 molar ratio resulted in the same effects as produced by SPwt alone, and preaddition of SP-3 or SP-4 to the vesicles did not affect membrane mixing induced by SPwt or SP-2, indicating that the nonfusogenic peptides were unable to interfere with the activity of fusogenic peptides under these conditions in vitro (data not shown).

The interaction of peptides with phospholipid vesicles was further investigated by measuring the ability of the peptides to induce leakage of calcein from PC/PE vesicles. The relative efficiency of these peptides in inducing leakage correlates with their fusogenic activity; the fusogenic peptides SPwt (16 and 13 amino acids) and SP-2 exhibited a high efficiency in inducing dye leakage, while the nonfusogenic peptides SP-3 and SP-4 did not destabilize the LUV envelope (Fig. 2B).

Conformation and orientation of the modified peptides. The peptides were deposited on the germanium crystal from a DMSO solution (1 mg/ml). At pH 7.4 and in the absence of lipid, the HIV-1 peptides adopt a β-sheet structure characterized by a maximum at 1,628 cm^{-1} (Fig. 3A). Estimation of the secondary structure by Fourier self-deconvolution and curve fitting confirmed this predominance of β-sheet structure (Table 1) for all the HIV-1 fusion peptides.

LUV of PC/PE (1:1 molar ratio) were incubated with the peptides for 1 h at 37°C, and the proteoliposomes were separated from the free peptides on a Sephadex G-50 column. In contrast to lipid-free peptide, proteoliposomes displayed FTIR spectra (Fig. 3B and C) with an intense band, centered at 1,735 cm^{-1}, corresponding to the COOH stretching vibration of the phospholipid ester bonds and a second band, centered at 1,652 cm^{-1}, corresponding to the amide I of peptides, indicating that the HIV-1 peptide preferentially adopted an α-helical conformation. There was a continuing shift to the α-helical conformation with the increase of the lipid-to-peptide ratio (Table 1).

The lipid-to-peptide ratio stated is the input ratio that was used to make the proteoliposomes before passage through the column, and the actual lipid-to-peptide ratio in the multilayer on the germanium plate has not been determined. However, the relative intensities of the peptide and lipid bands indicate a comparable degree of binding for the four peptides. This estimation was made by measuring the ratio $S_{amide}/S_{\nu(C=O)lipid}$ on the IR spectra [S_{amide} is the area of amide I measured between 1,680 and 1,600 cm^{-1}, and $S_{\nu(C=O)lipid}$ is the area of the lipid ν(C=O) band between 1,770 and 1,700 cm^{-1}] (9).

With the aid of the Fourier deconvolution and curve-fitting procedure, we found that the amide I band of HIV-1 fusion peptide is resolvable into three component bands with maxima near 1,665, 1,652, and 1,635 cm^{-1} (Fig. 4). The component near 1,652 cm^{-1} dominates the contours of the band (±85% of the total integrated intensity) and can be assigned to the amide I absorption of the α-helical domain of the peptide. The components near 1,665 and 1,635 cm^{-1} together contribute some 15% of the integrated intensity of amide I band and are attributable to the amide I vibrations of the non-α-helical domain of the peptide (which are probably the COOH and NH_2 extremities). The three modified peptides present, within the limits of experimental accuracy, the same conformation in the absence and in the presence of lipids as the wild-type fusion peptide does (Table 1).

To determine the orientation of the secondary structures with respect to the lipid bilayer, spectra were recorded with orthogonally polarized incident light. A larger absorbance at 90° indicates a dipole oriented preferentially close to the perpendicular of the membrane plane, and, conversely, a larger absorbance at 0° indicates a dipole much closer to the parallel of the membrane plane. The orientational distributions of SPwt and SP-2 peptides are distinctly different from the orientation of SP-3 and SP-4 (Fig. 5). The difference spectra 90° − 0° of SPwt and SP-2 reveal no deviation for the α-helix, suggesting that the α-helix is neither parallel nor perpendicular to the ATR element surface, as illustrated for the SP-2 peptide in Fig. 5A, while for SP-3 and SP-4, the 90° − 0° difference spectra show a negative deviation for the α-helix, suggesting an orientation parallel to the lipid membrane, as shown for SP-3 in Fig. 5B.

As described in Materials and Methods, the curve fitting applied to the polarized spectra in the amide I region allows the evaluation of the dichroic ratio R_{atr} ($A_{90°}/A_{0°}$) for the α-helical structure and the calculation of the angle between the long axis of the α-helix and the germanium plate. For the helical structure associated with SPwt and SP-2, the calculated dichroic ratio of 1.3 ± 0.04 corresponds to an angle of 50 ± 5° between the α-helix and the germanium plate. The dichroic ratios associated with the SP-3 and SP-4 helical structures are 0.85 ± 0.03, corresponding to an angle of 0 ± 5° (Table 1). To

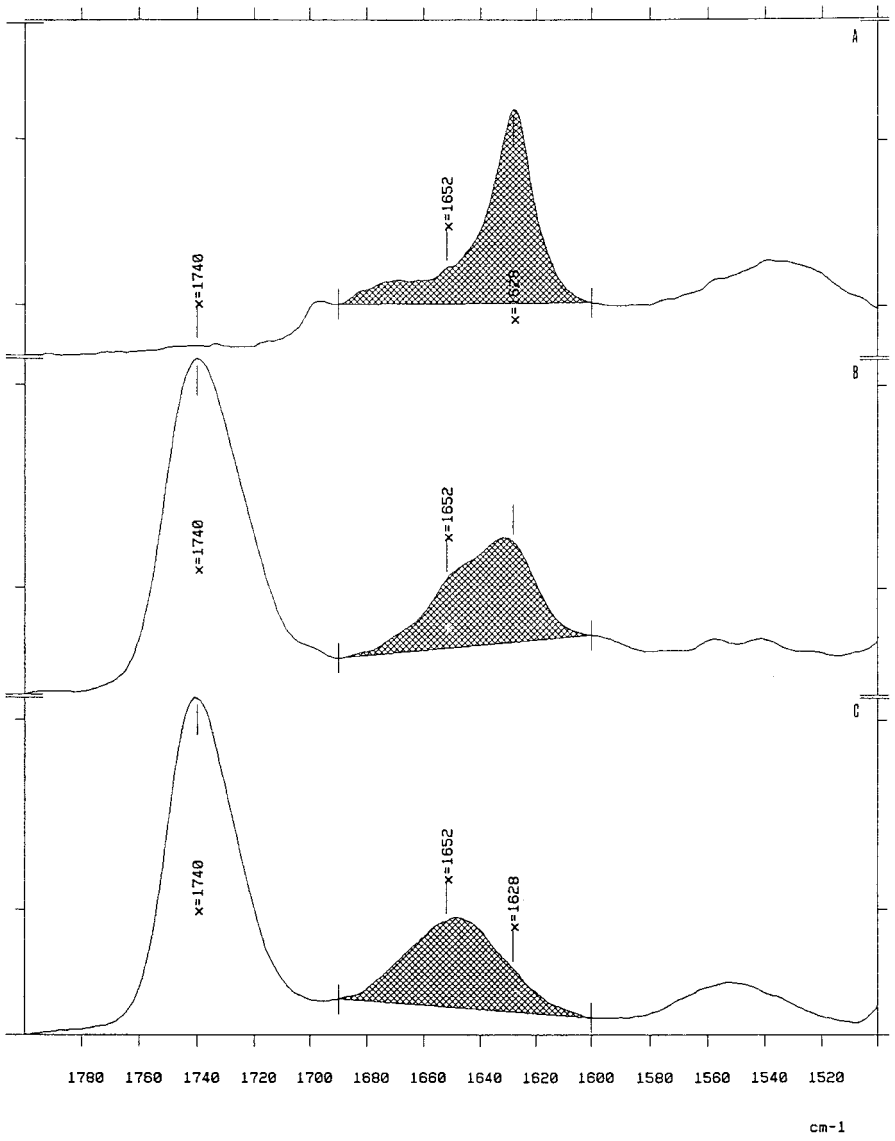

FIG. 3. ATR-FTIR spectra of SP-2 dissolved in DMSO (A) and inserted in LUV PC/PE at peptide-to-lipid molar ratios of 1:100 (B) and 1:200 (C).

determine these orientations, a 27° deviation angle between the α-helix axis and the C═O transition dipole moment described by Rothschild et al. (28) was taken into account by introducing an order parameter $S_{C=O} = (3\cos^2 27° - 1)/2$, so that $S_{helix} = S_{measured}/S_{C=O}$ (9, 11). The calculated angles between the helix axis and the bilayer are therefore minimum estimates, and an orientation of the helix axis closer to this perpendicular would result from considering other sources of disorder such as an imperfect parallelism between the bilayer and the germanium crystal surface.

Efforts have been made to characterize the orientation of the phospholipids in the bilayer in order to assess the overall membrane orientation on the germanium plate in the absence and the presence of peptide. In the absence of peptide, the peak of the phospholipid $\omega(CH_2)$ at 1,468 cm^{-1} that appears on the dichroic ratio spectra (obtained by subtracting the 0° spectrum from the 90° spectrum) as a negative deviation demonstrates that the phospholipid acyl chains are oriented almost perpendicular to the germanium plate; i.e., the bilayer lies parallel to the germanium plate (data not shown). The dichroic ratio of the $\omega(CH_2)$ vibration at 1,468 cm^{-1} is 0.80 ± 0.05 without or with peptide, and this is consistent with a well-ordered lipid film parallel to the plane of the germanium plate. The fact that peptide has no measurable effect on the lipid order is probably due to the low peptide-to-lipid molar ratio of 1:200 used in these experiments. Tamm and Tatulian (32) have demonstrated that only at peptide-to-lipid molar ratios up to 1:20 are small hydrophobic peptides able to disturb the orientational order of the lipid molecules to a significant degree.

DISCUSSION

The hydrophobic region located at the amino-terminal extremity of transmembrane envelope glycoproteins of several enveloped viruses (paramyxoviruses, orthomyxoviruses, and retroviruses) has been proposed to play a role in the fusion process and is referred to as the fusion peptide (for a review,

TABLE 1. Proportion of the different secondary structures of SPwt and mutant peptides in the absence and presence of LUV containing PC and PE at a 1:1 molar ratio

Sample[a]	FTIR secondary structure[b]			
	% α-helix (± 5%)	Dichroic ratio	% β-sheet (± 3%)	% Random (± 7%)
SPwt				
in DMSO	5		70	25
*r*L/P = 50	22	ND[c]	55	23
*r*L/P = 100	54	1.25	30	16
*r*L/P = 200	85	1.30	0	15
SP-2				
in DMSO	7		70	23
*r*L/P = 50	20	ND	50	25
*r*L/P = 100	55	1.30	30	15
*r*L/P = 200	85	1.32	0	15
SP-3				
in DMSO	7		60	33
*r*L/P = 50	13	ND	55	32
*r*L/P = 100	50	0.90	35	15
*r*L/P = 200	85	0.87	0	15
SP-4				
in DMSO	5		65	30
*r*L/P = 50	15	ND	60	25
*r*L/P = 100	55	0.83	30	15
*r*L/P = 200	85	0.85	0	15

[a] *r*L/P, lipid-to-peptide molar ratio before passage through a Sephadex G-50 column.
[b] The measurements were done after separation of the vesicle-bound peptide from free peptide on a Sephadex G-50 column.
[c] ND, not determined.

see reference 35). In HIV-1 and SIV, this hydrophobic domain is located at the N termini of gp41 and gp32.

Expression vectors for mutant glycoproteins with deletions of 1 to 7 amino acids of the N terminus of gp41 have recently been constructed and tested for their ability to induce membrane fusion after transfection of HeLa-T4$^+$ cells by electroporation and microinjection (29). The efficiency of cell-fusing activity decreased drastically with deletion of 3 amino acids or more, suggesting that a specific N-terminal structure is required for fusing activity even though the deletion of up to 2 amino acids can be tolerated (29).

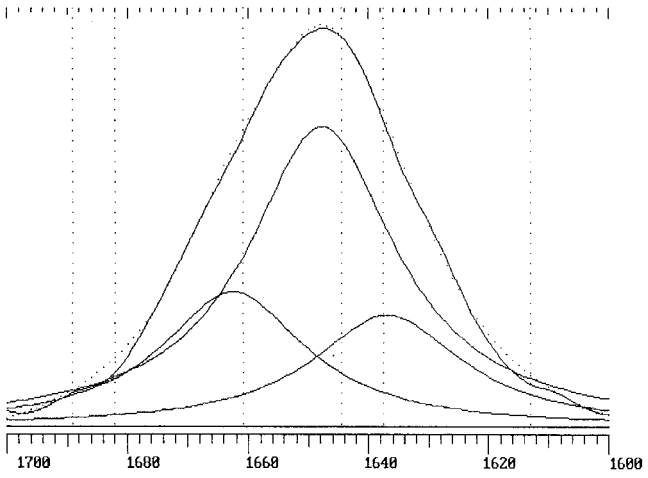

FIG. 4. FTIR spectra and curve fitting of the deuterated amide I band of SP-2 in the presence of lipid (LUV PC/PE lipid-to-peptide ratio, 200). The sum of the Lorentzian line shapes obtained is represented by the dotted spectrum. The vertical dotted lines define the regions associated with the different secondary structures. The frequency limits were as follows: 1,662 to 1,645 cm^{-1}, α-helix; 1,689 to 1,682 cm^{-1} and 1,637 to 1,613 cm^{-1}, β-sheet; 1,644.5 to 1,637 cm^{-1}, random; 1,682 to 1,662.5 cm^{-1}, β-turn.

Since different studies on SIV gp32 have revealed a correlation between the orientation of the fusion peptide in the lipid membrane and its fusogenic activity (14, 22), we have now analyzed synthetic peptides corresponding in sequence to the gp41 N termini of HIV-1 used by Schaal et al. (29) to ask whether the activity of these peptides and their interaction with lipid membranes correlates with the properties of the parent glycoproteins in vivo and with the membrane orientation of the peptides as predicted from our previous studies (14, 22).

The ability of the three mutant peptides to destabilize the lipid bilayer and to induce lipid mixing was tested and compared with the fusogenic activity of SPwt. SP-2 has an activity comparable to SPwt, while SP-3 and SP-4 have no capacity to destabilize the lipid bilayer or to induce membrane fusion. This loss of fusion activity cannot be ascribed to the shortening of the peptide per se, because Spwt13, a peptide equal in length to SP-3 but containing the N-terminal sequence of the 16-amino-acid Spwt, showed high fusion activity. These results with the model system are in good agreement with the in vivo data obtained by mutagenesis, which have also shown that the deletion of 2 amino acids has little effect on the fusogenic activity of gp41, while deletion of 3 and 4 amino acids drastically decreases the fusion activity in transfected HeLa-T4$^+$ cells (29).

To better understand the insertion mode of these peptides in the lipid membrane, we have used ATR-FTIR to determine their secondary structure in proteolipid complexes. The three mutant peptides were found to have the same secondary structure in lipid bilayers as the wild-type peptide did. All peptides undergo a conformational transition to an α-helical structure when interacting with lipid. This β-sheet–to–α-helix transition has previously been demonstrated by circular dichroism for synthetic peptides corresponding to the N-terminal extremity of influenza virus (18) and by IR spectroscopy for the fusion peptides of HIV-1 (19, 26) and SIV (20, 21).

Because of the similarity of the secondary structure of wild-type and mutant peptides, this parameter clearly cannot account for the large functional differences found between the wild-type and mutant peptides in vitro and between their parent glycoproteins in vivo. Another important physical parameter which could potentially discriminate between functional and nonfunctional fusion peptides is the orientation in the membrane of the α-helices. A useful method for determining the orientation of α-helices of proteins or peptides in the lipid bilayer is ATR-IR with polarized light (9, 10, 33). Applying this method to the peptides, we found that deletion of 3 or 4 residues significantly changes the orientation of the α-helix relative to the lipid bilayer, lowering the angle relative to the plane of the membrane close to the parallel. This is in contrast to the oblique orientation of the wild-type peptide and SP-2. Thus, as subtle a change in sequence as the loss of 1 amino acid residue (from SP-2 to SP-3) can result in significant changes of the orientation of the helix, and this correlates with the change in the membrane fusion activity in vitro observed in this study and with the previously observed differences in fusion activity of the parent glycoproteins in vivo (29).

The results suggest that the oblique angle at which the hydrophobic fusion peptide is inserted into the lipid bilayer is an important parameter for its ability to destabilize the lipid organization and to promote membrane fusion. This further supports the correlation between membrane orientation and fusion that has previously been observed with SIV fusion

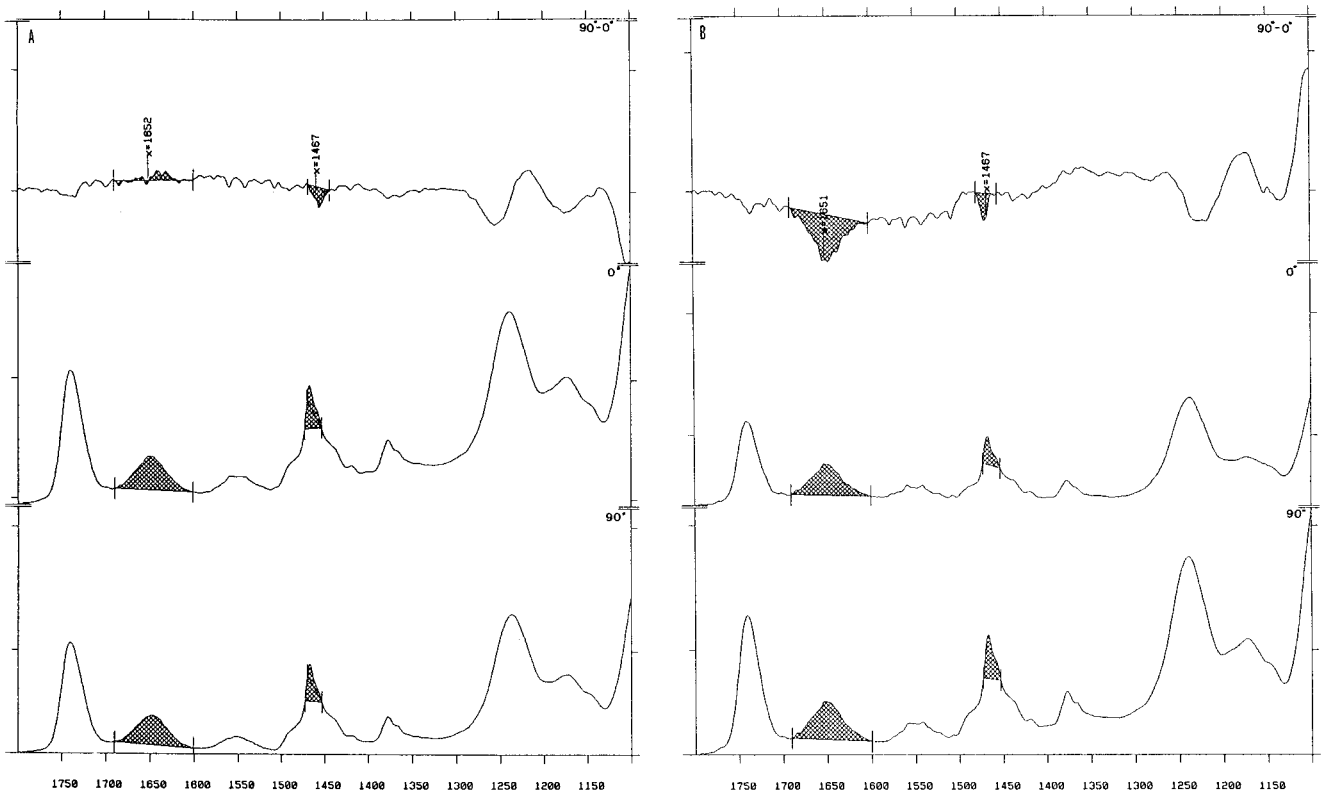

FIG. 5. ATR-FTIR spectra of SP-2 inserted in LUV PC/PE (A) and SP-3 inserted in LUV PC/PE (B), recorded with 90° (bottom) and 0° (middle) polarization. The dichroism spectrum obtained by subtracting the 0° from the 90° recorded spectra is plotted at the top of the figure and expanded threefold in the ordinate direction. The bars indicate the protein amide I bands in the region of 1,600 to 1,700 cm^{-1} and the phospholipid $\omega(CH_2)$ at 1,467 cm^{-1}. The difference spectra are normalized to each other by setting to zero the net integral of the intensities of the ester C═O stretching bands of the Sn1 and Sn2 chains in the 1,710- to 1,760-cm^{-1} region of the difference spectrum.

peptides (22) and with mutations introduced into the fusion peptide of the entire SIV glycoprotein (14). A possible mechanism by which peptides inserted into membranes at an oblique angle may perturb bilayer packing is by increasing the negative curvature strain, thereby favoring the formation of inverted phases. There is some evidence that viral fusion peptides of SIV and influenza virus may promote fusion by this mechanism of phase destabilization (3, 4).

The good correlation observed between the in vitro and in vivo experiments confirms the complementarity and the potential of the two methods for examining the mechanisms by which peptide region of a transmembrane protein induce lipid bilayer fusion. Moreover, the similarity observed in the HIV and SIV systems (22) suggests the existence of a common fusion mechanism induced by the fusion peptides.

ACKNOWLEDGMENTS

This work was performed with the financial support of FNRS (Fonds National de la Recherche Scientifique), of the Commission of the European Communities (contract CT 920324), and of ARC (Action de Recherches Concertées).

REFERENCES

1. **Bosch, M., P. Earl, K. Fargnoli, S. Picciafuoco, F. Giombini, F. Wong Staal, and G. Franchini.** 1989. Identification of the fusion peptide of primate immunodeficiency viruses. Science **244:**694–697.
2. **Cabiaux, V., R. Brasseur, R. Wattiez, P. Falmagne, J.-M. Ruysschaert, and E. Goormaghtigh.** 1989. Secondary structure of DT and its fragments interacting with acidic liposomes studied by polarized infrared spectroscopy. J. Biol. Chem. **264:**4928–4938.
3. **Epand, R. F., I. Martin, J.-M. Ruysschaert, and R. M. Epand.** 1994. Membrane orientation of the SIV fusion peptides determines its effect on bilayer stability and ability to promote membrane fusion. Biochem. Biophys. Res. Commun. **205:**1938–1943.
4. **Epand, R. M., and R. F. Epand.** 1994. Relationship between the infectivity of influenza virus and the ability of its fusion peptide to perturb bilayers. Biochem. Biophys. Res. Commun. **202:**1420–1425.
5. **Freed, E. D., and R. Risser.** 1990. The role of the HIV envelope glycoproteins in cell fusion and the pathogenesis of AIDS. Bull. Inst. Pasteur **88:**73–110.
6. **Fringeli, U. R., and M. H. Günthard.** 1981. Infrared membrane spectroscopy, p. 270–332. *In* E. Grell (ed.), Membrane spectroscopy. Springer-Verlag, Berlin.
7. **Gallaher, W. R., J. M. Ball, R. F. Garry, M. C. Griffin, and R. C. Montelaro.** 1989. A general model for the transmembrane proteins of HIV and other retroviruses. AIDS Res. Hum. Retroviruses **5:**431–440.
8. **Gething, M.-J., R. Doms, D. York, and J. White.** 1986. Studies on the mechanism of membrane fusion: site-specific mutagenesis of the hemagglutinin of influenza virus. J. Cell Biol. **102:**11–23.
9. **Goormaghtigh, E., V. Cabiaux, and J.-M. Ruysschaert.** 1990. Secondary structure and dosage of soluble and membrane proteins by attenuated total reflection Fourier-transform infrared spectroscopy on hydrated film. Eur. J. Biochem. **193:**409–420.
10. **Goormaghtigh, E., V. Cabiaux, and J. M. Ruysschaert.** 1994. Determination of soluble and membrane protein structure by Fourier transformed infrared spectroscopy. Subcell. Biochem. **23:**329–450.
11. **Gremlich, H. U., U. P. Fringeli, and R. Schwyzer.** 1983. Conformational changes of adrenocorticotropin peptides upon interaction with lipid membranes revealed by infrared attenuated total reflection spectroscopy. Biochemistry **22:**4257–4264.
12. **Hong, K., T. Yoshimura, and D. Papahadjopoulos.** 1985. Interaction of clathrin with liposomes: pH-dependent fusion of phospholipid membranes induced by clathrin. FEBS Lett. **191:**17–23.
13. **Hope, M. J., M. B. Bally, G. Webb, and P. R. Cullis.** 1985. Production of large unilamellar vesicles by a rapid extrusion procedure: characterization of size distribution, entrapped volume and ability to maintain a membrane potential. Biochim. Biophys. Acta **812:**55–65.

14. **Horth, M., B. Lambrechts, C. Marinee, F. Bex, C. Thiriart, J.-M. Ruysschaert, A. Burny, and R. Brasseur.** 1991. Theoretical and functional analysis of the HIV fusion peptide. EMBO J. **10:**2747–2755.
15. **Kauppinen, J. K., D. J. Moffat, D. G. Cameron, and H. Mantsch.** 1981. Noise in Fourier self-deconvolution. Appl. Opt. **20:**1866–1879.
16. **Kowalski, M., J. Potz, L. Basiripour, T. Dorfman, W. Goh, E. Terwilliger, A. Dayton, C. Rosen, W. Haseltine, and J. Sodroski.** 1987. Functional regions of the envelope glycoprotein of HIV type-1. Science **237:**1351–1355.
17. **Krimm, S., and J. Bandekar.** 1986. Vibrational spectroscopy and conformation of peptides, polypeptides and proteins. Adv. Protein Chem. **38:**181–264.
18. **Lear, J. D., and W. DeGrado.** 1987. Membrane binding and conformational properties of peptides representing the NH2 terminus of influenza HA2. J. Biol. Chem. **262:**6500–6505.
19. **Martin, I., F. Defrise-Quertain, E. Decroly, T. Saermark, M. Vandenbranden, R. Brasseur, and J.-M. Ruysschaert.** 1992. Orientation of the NH2-terminal HIV-1 gp41 peptide in fused and aggregated liposomes. Biochim. Biophys. Acta **1145:**124–133.
20. **Martin, I., F. Defrise-Quertain, V. Mandiau, T. Saermark, A. Burny, R. Brasseur, J.-M. Ruysschaert, and M. Vandenbranden.** 1991. Fusogenic activity of SIV peptides located in the gp32 NH2-terminal domain. Biochem. Biophys. Res. Commun. **175:**872–879.
21. **Martin, I., F. Defrise-Quertain, N.-M. Nielsen, T. Saermark, M. Vandenbranden, R. Brasseur, and J.-M. Ruysschaert.** 1992. Study of the interaction between lipids and the NH2-terminal peptide of SIV fusion protein. Adv. Membr. Fluid. **6:**365–376.
22. **Martin, I., M. C. Dubois, F. Defrise-Quertain, T. Saermark, A. Burny, R. Brasseur, and J. M. Ruysschaert.** 1994. Correlation between fusogenicity of synthetic modified peptides corresponding to the NH_2-terminal extremity of SIV gp32 and their mode of insertion into the lipid bilayer: an infrared spectroscopy study. J. Virol. **68:**1139–1148.
23. **Msrny, R., J. Volwerk, and H. Griffith.** 1986. A simplified procedure for lipid phosphorus analysis shows that digestion rates vary with phospholipid structure. Chem. Phys. Lipids **39:**185–191.
24. **Murata, M., Y. Sugahara, S. Takahashi, and S. Ohnishi.** 1987. pH-dependent membrane fusion activity of a synthetic 20 amino-acid peptide with the same sequence as that of the hydrophobic segment of influenza virus hemagglutinin. J. Biochem. **102:**957–962.
25. **Pereira, F., F. Goni, and J. Nieva.** 1995. Liposome destabilization induced by the HIV-1 fusion peptide. Effect of a single amino acid substitution. FEBS Lett. **362:**243–246.
26. **Rafalski, M., J. D. Lear, and W. DeGrado.** 1990. Phospholipid interactions of synthetic peptides representing the N-terminus of HIV gp41. Biochemistry **29:**7917–7922.
27. **Rafalski, M., A. Ortiz, A. Rockwell, L. van Ginkel, J. Lear, W. DeGrado, and J. Wilschut.** 1991. Membrane fusion activity of the influenza virus hemagglutinin: interaction of HA2 N-terminal peptides with phospholipid vesicles. Biochemistry **30:**10211–10220.
28. **Rothschild, K., R. Sanches, T. Hsiao, and N. Clark.** 1980. Infrared absorption of photoreceptor and purple membranes. Biophys. J. **31:**53–60.
29. **Schaal, H., M. Klein, P. Gehrmann, O. Adams, and A. Scheid.** 1995. Requirement of N-terminal amino acid residues of gp41 for human immunodeficiency virus type 1-mediated cell fusion. J. Virol. **69:**3308–3314.
30. **Struck, D. K., D. Hoekstra, and R. Pagano.** 1981. Use of resonance energy transfer to monitor membrane fusion. Biochemistry **20:**4093–4099.
31. **Susi, H., and D. M. Byler.** 1986. Calculation of the secondary structure of protein by deconvoluted FTIR spectra. Biopolymers **25:**459–487.
32. **Tamm, L., and S. Tatulian.** 1993. Orientation of functional and non functional PTS permease signal sequences in lipid bilayer. A polarized attenuated total reflection infrared study. Biochemistry **32:**7720–7726.
33. **Vandenbussche, G., A. Clerckx, M. Clerckx, J. Curstedt, J. Johansson, H. Jörnvall, and J. M. Ruysschaert.** 1992. Secondary structure and orientation of the surfactant protein SP-B in a lipid environment. A FTIR spectroscopy study. Biochemistry **31:**9169–9176.
34. **Wharton, S. A., S. Martin, R. Ruigrok, J. Skehel, and D. Wiley.** 1988. Membrane fusion by peptide analogues of influenza virus hemagglutinin. J. Gen. Virol. **69:**1847–1857.
35. **White, J.** 1990. Viral and cellular membrane fusion proteins. Annu. Rev. Physiol. **52:**675–697.